Anomalous magnetohydrodynamics with longitudinal boost invariance and chiral magnetic effect

Irfan Siddique, Ren-jie Wang, Shi Pu, and Qun Wang
Department of Modern Physics, University of Science and Technology of China, Hefei 230026, China

(Received 7 May 2019; published 28 June 2019)

We study relativistic magnetohydrodynamics with longitudinal boost invariance in the presence of chiral magnetic effects and finite electric conductivity. With initial magnetic fields parallel or antiparallel to electric fields, we derive the analytic solutions of electromagnetic fields and the chiral number and energy density in an expansion of several parameters determined by initial conditions. The numerical solutions show that such analytic solutions work well in weak fields or large chiral fluctuations. We also discuss the properties of electromagnetic fields in the laboratory frame.

DOI: 10.1103/PhysRevD.99.114029

I. INTRODUCTION

Recently some novel transport phenomena of chiral (massless) fermions in strong electromagnetic (EM) fields have been extensively studied in relativistic heavy ion collisions and condensed matter physics. One of them is the chiral magnetic effect (CME): an electric current can be induced by the strong magnetic field when the numbers of left- and right-handed fermions are not equal [1–3]. Similarly the strong magnetic field can also lead to the chiral separation effect for the chiral charge current. These effects are associated with the chiral anomaly and can be described by chiral kinetic equations (CKE). The CKE are derived from various approaches, e.g., the path integral [4–6], the Hamiltonian approach [7,8], the quantum kinetic theory via Wigner functions [9–17], and the world-line formalism [18,19]. The chiral separation can also be induced by an electric field, which is called the chiral electric separation effect (CESE) [20–23]. If the electric field is perpendicular to the magnetic field, a Hall current for chiral fermions is expected, which is called chiral Hall separation effect [23]. The chiral particle production in strong EM fields is found to be directly connected to the Schwinger mechanism [24,25], and similar calculation has been done analytically via the world-line formalism [26] and Wigner functions [27]. Recent reviews about chiral transport phenomena can be found in Refs. [28–31].

The chiral transport phenomena are expected to have observables in relativistic heavy ion collisions in which very strong magnetic fields of the order $B \sim 10^{18}$ G are produced [32–35]. At the very early stage of the quark-gluon plasma (QGP), the topological fluctuations in non-Abelian gauge fields give rise to the imbalance of chirality from event to event (event by event). Such an imbalance of chirality may lead to the charge separation with respect to the reaction plane in heavy ion collisions. The STAR collaboration has observed the charge separation in $\mathrm{Au}+\mathrm{Au}$ collisions [36,37]. However, due to the huge backgrounds from collective flows [38,39] it is a challenge to extract the weak CME signal from the overwhelming background. It is expected that the ongoing isobar collision experiment at STAR may shed light on the CME signal (see e.g., Ref. [40] for discussions on isobar collisions).

In order to extract the CME signal, we need the precise simulation of the QGP evolution in the time-evolving EM field. One approach is through the simulation of the CKE. Very recently, the boost invariant formulation of the CKE has been done with the chiral circular displacement introduced [41]. The CKE has been solved numerically in heavy ion collisions [42,43]. Another approach is the classical statistical simulation based on solving the coupled equations of Yang-Mills and Dirac applied to heavy ion collisions [44–46]. Besides the relativistic hydrodynamic is a widely used model in relativistic heavy ion collisions.

The relativistic hydrodynamic model is one of the main approaches to the QGP evolution [47–53]. A natural extension of the hydrodynamic model in the presence of the magnetic field is the magentohydrodynamics (MHD), which is hydrodynamics coupled with Maxwell's equations. The ideal MHD equations with longitudinal boost invariance and a transverse magnetic field have been calculated [54,55], where the magnetic field decays as $\sim 1/\tau$ with τ being the proper time, much slower than in vacuum [2]. The magnetization effect has also been systematically studied [54]. Later the calculation was extended to $2+1$ dimensions [56,57]. There is an enhancement of the elliptic flow v_2 of π^-

from the external magnetic field [58]. Recently the MHD with the longitudinal boost invariance has been extended to include the finite conductivity in the Gubser flow [59]. Readers may look at Ref. [60] for recent numerical simulations of the ideal MHD.

In this work, we consider the relativistic MHD in the presence of the CME and finite conductivity. Usually the numerical simulations of MHD with the CME could be very unstable because of chirality instability [61]. Therefore stable analytic solutions in some special cases are very important for providing a test of numerical simulations and a simple physical picture for such a complicated process. As a first attempt, we consider the MHD with the longitudinal boost invariance. To avoid the acceleration of the fluid by the EM field, we assume an electric charge neutral fluid. We then search for the EM fields that can keep the Bjorken fluid velocity unchanged. It is very similar to the case of the force-free magnetic field discussed in classical electrodynamics [62,63]. To solve the coupled equations of the anomalous conservation equation and Maxwell's equations, we assume that the terms proportional to the anomaly constant (proportional to the Planck constant $\hbar$) are perturbations, this is equivalent to an expansion in $\hbar$. We compare our approximate analytic solutions with the numerical results. Finally we compute the EM field in the laboratory frame and discuss the coupling between the EM field and the chiral current.

The organization of the paper is as follows. In Sec. II, we give a brief review for the relativistic MHD with the CME. In Sec. III, we assume the form of the fluid velocity in longitudinal boost invariance. We choose a configuration of the EM field that is orthogonal to the fluid velocity. In Secs. IV A and IV B, we solve Maxwell's equations coupled with the anomalous conservation equation for the chiral charge. We obtain the approximate analytic solutions for two different equations of state. We compare our approximate analytic solutions with numerical ones. In Sec. IV C, we compute the EM field in the laboratory frame to show the consistence with previous results. Finally we make a summary of our results in Sec. V.

Throughout this work, we use the metric $g_{\mu\nu}=\mathrm{diag}\{+,-,-,-\}$; thus, the fluid velocity satisfies $u^\mu u_\mu=1$, and the orthogonal projector to the fluid four-velocity is $\Delta^{\mu\nu}=g^{\mu\nu}-u^\mu u^\nu$. We also choose the Levi-Civita tensor satisfying $\epsilon^{0123}=-\epsilon_{0123}=+1$ and $\epsilon^{\mu\nu\alpha\beta}\epsilon_{\mu\nu\rho\sigma}=-2!(g^\alpha_\rho g^\beta_\sigma-g^\alpha_\sigma g^\beta_\rho)$.

II. ANOMALOUS MAGNETOHYDRODYNAMICS

In this section, we give a brief preview to the relativistic MHD with CME, which is called anomalous magnetohydrodynamics. The MHD equations consist of conservation equations and Maxwell's equations (see, e.g., Refs. [54–57,64–66] for details). The energy-momentum conservation equation reads

$$\partial_\mu T^{\mu\nu}=0, \tag{1}$$

where $T^{\mu\nu}$ is the energy-momentum tensor including the contributions from the fluid and the EM fields

$$T^{\mu\nu}=T^{\mu\nu}_F+T^{\mu\nu}_{\mathrm{EM}}. \tag{2}$$

The fluid part has the usual form,

$$T^{\mu\nu}_F=\varepsilon u^\mu u^\nu-(p+\Pi)\Delta^{\mu\nu}+\pi^{\mu\nu}, \tag{3}$$

where ε and p are the energy density and pressure, respectively, $u^\mu=\gamma(1,\mathbf{v})$ is the fluid velocity satisfying $u^\mu u_\mu=1$, $\Delta^{\mu\nu}=g^{\mu\nu}-u^\mu u^\nu$ is the projector, and Π and $\pi^{\mu\nu}$ are bulk viscous pressure and shear viscous tensor, respectively. For simplicity, we neglect viscous effects in this paper, i.e., $\Pi=\pi^{\mu\nu}=0$. The EM field part of the energy-momentum tensor reads

$$T^{\mu\nu}_{\mathrm{EM}}=-F^{\mu\lambda}F^\nu_\lambda+\frac{1}{4}g^{\mu\nu}F^{\rho\sigma}F_{\rho\sigma}. \tag{4}$$

One can introduce the four-vector form of the electric and magnetic fields in terms of the fluid velocity

$$E^\mu=F^{\mu\nu}u_\nu,\qquad B^\mu=\frac{1}{2}\epsilon^{\mu\nu\alpha\beta}u_\nu F_{\alpha\beta}, \tag{5}$$

which satisfies $u^\mu E_\mu=0$ and $u^\mu B_\mu=0$ meaning that both E^μ and B^μ are spacelike. Then, the EM field strength tensor can be put into the form

$$F^{\mu\nu}=E^\mu u^\nu-E^\nu u^\mu+\epsilon^{\mu\nu\alpha\beta}u_\alpha B_\beta. \tag{6}$$

Inserting the above formula into Eq. (4), we obtain the complete form of the energy-momentum tensor from Eq. (2),

$$\begin{aligned}T^{\mu\nu}=&(\varepsilon+p+E^2+B^2)u^\mu u^\nu-\left(p+\frac{1}{2}E^2+\frac{1}{2}B^2\right)g^{\mu\nu}\\&-E^\mu E^\nu-B^\mu B^\nu-u^\mu\epsilon^{\nu\lambda\alpha\beta}E_\lambda B_\alpha u_\beta-u^\nu\epsilon^{\mu\lambda\alpha\beta}E_\lambda B_\alpha u_\beta,\end{aligned} \tag{7}$$

where E and B are defined by

$$E^\mu E_\mu=-E^2,\qquad B^\mu B_\mu=-B^2. \tag{8}$$

The conservation equations are

$$\begin{aligned}\partial_\mu j^\mu_e&=0,\\\partial_\mu j^\mu_5&=-e^2CE\cdot B,\end{aligned} \tag{9}$$

where j_e^μ is the electric charge current and j_5^μ is the chiral (axial) charge current. Note that the chiral anomaly term appears in the second line of Eq. (9) with $C = 1/(2\pi^2)$. These currents can be decomposed into three parts,

$$j_e^\mu = n_e u^\mu + \sigma E^\mu + \xi B^\mu,$$
$$j_5^\mu = n_5 u^\mu + \sigma_5 E^\mu + \xi_5 B^\mu, \tag{10}$$

where n_e and n_5 are the electric and chiral charge density, respectively, σ and σ_5 are the electric and chiral electric conductivity, respectively [20,21,23], and ξ and ξ_5 are associated with the CME and CESE [3,9,10], which are given by

$$\xi = eC\mu_5, \qquad \xi_5 = eC\mu_e. \tag{11}$$

For simplicity, we neglect all other dissipative effects in j_e^μ and j_5^μ such as the heat conducting flow. The chiral electric conductivity σ_5 is usually parametrized as $\sigma_5 \propto \mu_e\mu_5$ in the small μ_e and μ_5 limit [20,21,23].

Maxwell's equations can be put into the following form,

$$\partial_\mu F^{\mu\nu} = j_e^\nu, \tag{12}$$

$$\partial_\mu(\epsilon^{\mu\nu\alpha\beta}F_{\alpha\beta}) = 0. \tag{13}$$

To close the system of equations, we need to choose the equations of state (EoS) for the thermodynamic quantities. In the dense limit with high chemical potentials, we use

$$\varepsilon = c_s^{-2}p,$$
$$n_e = a\mu_e(\mu_e^2 + 3\mu_5^2),$$
$$n_5 = a\mu_5(\mu_5^2 + 3\mu_e^2), \tag{14}$$

where a is a dimensionless constant and c_s is the speed of sound also taken as a constant. On the other hand, in the hot limit with high temperatures, we use

$$\varepsilon = c_s^{-2}p,$$
$$n_e = a\mu_e T^2,$$
$$n_5 = a\mu_5 T^2, \tag{15}$$

where a is again a dimensionless constant. Note that the value of a in Eq. (15) is different from that in Eq. (14). For the ideal fluid, we have $a = 1/(3\pi^2)$ and $a = 1/3$ for Eq. (14) and (15), respectively [9,67].

Usually the electric field would accelerate charged particles and the charged fluid. To avoid such a problem, we simply set the chemical potential for electric charge vanishing, $\mu_e = 0$, which also leads to $n_e = \sigma_5 = \xi_5 = 0$. Such a condition means the fluid is neutral: the number of positively charged particles is the same as that of negatively charged particles. Actually we look for a special configuration of EM fields coupled with the media, very similar to the force-free case in classical electrodynamics. In Sec. IV C, we discuss the details and check the consistence of this assumption.

Here are the whole system of equations we are going to solve: conservation equations (1) and (9), Maxwell's equations (12) and (13), constitutive equations (7), (6), and (10), and equations of state (14) and (15).

III. EQUATIONS WITH LONGITUDINAL BOOST INVARIANCE

We assume that the fluid has longitudinal boost invariance. It is convenient to introduce the Milne coordinates $z = \tau\sinh\eta$ and $t = \tau\cosh\eta$, with $\tau = (t^2 - z^2)^{1/2}$ being the proper time and $\eta = \frac{1}{2}\ln[(t+z)/(t-z)]$ being the space-time rapidity. The fluid velocity with longitudinal boost invariance can be written as [68]

$$u^\mu = (\cosh\eta, 0, 0, \sinh\eta) = \gamma(1, 0, 0, z/t), \tag{16}$$

where $\gamma = \cosh\eta$ is the Lorentz contraction factor.

For simplicity we neglect the EM field in the longitudinal direction, so the general form of the EM field satisfying $u\cdot E = u\cdot B = 0$ is

$$E^\mu = (0, E\cos\zeta, E\sin\zeta, 0),$$
$$B^\mu = (0, B\cos\varphi, B\sin\varphi, 0), \tag{17}$$

where ζ and φ are the azimuthal angle of the electric and magnetic field in the transverse plane, respectively. To search for possible analytic solutions, we assume that E^μ and B^μ will always be in the transverse plane and that E, B, ζ, φ are only functions of τ. We can further simplify the problem by assuming that E^μ and B^μ are parallel or antiparallel. Without loss of generality, the EM field can be put in the y direction,

$$E^\mu = (0, 0, \chi E(\tau), 0), \qquad B^\mu = (0, 0, B(\tau), 0), \tag{18}$$

where $\chi = \pm 1$. We check the self-consistence of these assumptions after we find the solution in Sec. IV C. Note that the authors of Ref. [69] have found another possible configuration of the EM fields in the absence of the chiral magnetic effect, in which the direction of the electric and magnetic field depends on η. As this configuration is irrelevant to the heavy ion collisions, we do not consider it in this paper.

By projecting the energy-momentum conservation equation (1) onto the spatial direction, $\Delta_{\mu\alpha}\partial_\nu T^{\mu\nu} = 0$, we obtain the acceleration of the fluid velocity,

$$(u\cdot\partial)u_\alpha=\frac{1}{(\varepsilon+p+E^2+B^2)}\left[\Delta_\alpha^\nu\partial_\nu\left(p+\frac{1}{2}E^2+\frac{1}{2}B^2\right)+\Delta_{\mu\alpha}(E\cdot\partial)E^\mu+E_\alpha(\partial\cdot E)+\Delta_{\mu\alpha}(B\cdot\partial)B^\mu+B_\alpha(\partial\cdot B)+\epsilon^{\nu\lambda\rho\sigma}E_\lambda B_\rho u_\sigma(\partial_\nu u_\alpha)+(\partial\cdot u)\epsilon_{\alpha\lambda\rho\sigma}E^\lambda B^\rho u^\sigma+\Delta_{\mu\alpha}(u\cdot\partial)\epsilon^{\mu\lambda\rho\sigma}E_\lambda B_\rho u_\sigma\right]. \tag{19}$$

According to our assumption that the electric and magnetic field are constant in transverse coordinates (x, y), we have $(E\cdot\partial)E^\mu=(\partial\cdot E)=(B\cdot\partial)B^\mu=(\partial\cdot B)=0$. Also, if p, E^μ and B^μ are only the functions of τ, the first term inside the square brackets is vanishing. So we obtain the non-acceleration of the fluid velocity

$$(u\cdot\partial)u_\alpha=0, \tag{20}$$

which means that the fluid velocity always takes the value in Eq. (16). This is consistent to the previous assumption that the fluid is charge neutral.

The energy conservation equation can be obtained by a contraction of u_μ with Eq. (1) or $u_\mu\partial_\nu T^{\mu\nu}=0$,

$$(u\cdot\partial)\left(\varepsilon+\frac{1}{2}E^2+\frac{1}{2}B^2\right)+(\varepsilon+p+E^2+B^2)(\partial\cdot u)=u_\mu(E\cdot\partial)E^\mu+u_\mu(B\cdot\partial)B^\mu+\epsilon^{\nu\lambda\alpha\beta}\partial_\nu(E_\lambda B_\alpha u_\beta)+u_\mu(u\cdot\partial)\epsilon^{\mu\lambda\alpha\beta}E_\lambda B_\alpha u_\beta. \tag{21}$$

With Eq. (18), the above equation is reduced to

$$(u\cdot\partial)\left(\varepsilon+\frac{1}{2}E^2+\frac{1}{2}B^2\right)+(\varepsilon+p+E^2+B^2)(\partial\cdot u)=0. \tag{22}$$

Now we look at Maxwell's equations. Inserting Eq. (18) for the EM fields into Eq. (12) yields for $\nu=y$

$$\frac{d}{d\tau}E+\frac{1}{\tau}E+\sigma E+\chi\xi B=0, \tag{23}$$

where we have used $d/d\tau\equiv(u\cdot\partial)$. For other indices $\nu=t, x, z$, we obtain identities using $\mu_e=0$ and $n_e=0$. Similarly, from Eq. (13), we obtain for $\nu=y$

$$\frac{d}{d\tau}B+\frac{B}{\tau}=0. \tag{24}$$

For other indices $\nu=t, x, z$, we obtain identities using $\mu_e=0$ and $n_e=0$.

Using the simplified Maxwell's equations (23) and (24), we can rewrite Eq. (22) into a compact form

$$\frac{d}{d\tau}\varepsilon+(\varepsilon+p)\frac{1}{\tau}-\sigma E^2-\chi\xi EB=0. \tag{25}$$

This equation can also be derived by rewriting Eq. (1) as

$$\partial_\mu T_F^{\mu\nu}=-\partial_\mu T_{\rm EM}^{\mu\nu}=F^{\nu\lambda}j_{e\lambda}. \tag{26}$$

Contracting the above equation with u_ν yields $u_\nu\partial_\mu T_F^{\mu\nu}=-E^\lambda j_{e\lambda}$, which is consistent with Eq. (25).

From Eq. (9) and using $\mu_e=0$, the (anomalous) conservation equation of the chiral charge can be reduced to

$$\frac{d}{d\tau}n_5+\frac{n_5}{\tau}=e^2C\chi EB. \tag{27}$$

The conservation equation for j_e^μ is automatically satisfied with $\mu_e=0$ and E^μ, B^μ taking the form of Eq. (18).

Before we end this section, we make some remarks about the simplified equations with longitudinal boost invariance. To enforce the fluid velocity not accelerated, the EM field is assumed to take the form as Eq. (18). Using Maxwell's equations the energy conservation equation $u_\mu\partial_\nu T^{\mu\nu}=0$ is reduced to Eq. (25). The momentum conservation equation $\Delta_{\mu\alpha}\partial_\nu T^{\mu\nu}=0$ is reduced to Eq. (20), meaning that the fluid velocity always takes value in (16). Maxwell's equations (12) and (13) are simplified to Eqs. (23) and (24). The chiral charge conservation equation in Eq. (9) is simplified to Eq. (27).

IV. ANALYTIC SOLUTIONS

We use the nonconserved charges method [69,70] to solve Eqs. (23), (24), (25), and (27) with the EoS (14) or (15).

The nonconserved charges method is to solve the equation for $f(\tau)$ in the following form,

$$\frac{d}{d\tau}f(\tau)+m\frac{f(\tau)}{\tau}=f(\tau)\frac{d}{d\tau}\lambda(\tau), \tag{28}$$

where m is a constant and $\lambda(\tau)$ is a known function. The general solution is

$$f(\tau)=f(\tau_0)\exp\left[\lambda(\tau)-\lambda(\tau_0)\right]\left(\frac{\tau_0}{\tau}\right)^m, \tag{29}$$

where τ_0 is an initial proper time and $f(\tau_0)$ is determined by an initial value at τ_0. In this paper we rewrite Eqs. (23), (24), (25), and (27) in the form of Eq. (28) and obtain the solutions in the form of Eq. (29).

Note that generally f can also be a function of rapidity η [69,70]. However, in this paper we focus on the central rapidity region in heavy ion collisions, which implies $\eta\simeq 0$ with longitudinal boost invariance; therefore we do not consider the rapidity dependence.

From Eq. (24), we immediately obtain

$$B(\tau) = B_0 \frac{\tau_0}{\tau}, \tag{30}$$

where $B_0 = B(\tau_0)$ is the initial value of the magnetic field. We see that the proper time behavior of the magnetic field seems to be the same as the case without the CME [54–56]. But we show in Sec. IV C that the contribution from the CME and finite conductivity to the EM field appear in the lab frame.

A. EoS (14)

For the EoS (14), we solve Eq. (23) with Eq. (27) to obtain $n_5(\tau)$ and $E(\tau)$. Then we insert $n_5(\tau)$ and $E(\tau)$ into Eq. (25) to obtain the energy density $\varepsilon(\tau)$.

We need to put Eqs. (23) and (27) into the form of Eq. (28),

$$\begin{aligned} \frac{d}{d\tau}E + \frac{E}{\tau} &= E\frac{d}{d\tau}\mathcal{E}, \\ \frac{d}{d\tau}n_5 + \frac{n_5}{\tau} &= n_5\frac{d}{d\tau}\mathcal{N}, \end{aligned} \tag{31}$$

where

$$\begin{aligned} \frac{d}{d\tau}\mathcal{E} &= -\sigma - \chi\xi\frac{B}{E}, \\ \frac{d}{d\tau}\mathcal{N} &= \frac{e^2 C\chi EB}{n_5}, \end{aligned} \tag{32}$$

and ξ is given by Eq. (11) and depends on n_5 through the EoS (14). Following Eq. (29), the formal solutions are in the form

$$\begin{aligned} n_5(\tau) &= n_{5,0}\exp\left[\mathcal{N}(\tau) - \mathcal{N}(\tau_0)\right]\frac{\tau_0}{\tau}, \\ E(\tau) &= E_0\exp\left[\mathcal{E}(\tau) - \mathcal{E}(\tau_0)\right]\frac{\tau_0}{\tau}, \end{aligned} \tag{33}$$

where $n_{5,0} = n_5(\tau_0)$ and $E_0 = E(\tau_0)$. Inserting the above $n_5(\tau)$ and $E(\tau)$ as well as $B(\tau)$ in Eq. (30) into Eq. (32), we obtain

$$\begin{aligned} \frac{d}{d\tau}x &= -\sigma x - \frac{a_1}{\tau_0}\left(\frac{\tau_0}{\tau}\right)^{1/3} y^{1/3}, \\ \frac{d}{d\tau}y &= a_2\frac{x}{\tau}, \end{aligned} \tag{34}$$

where we have introduced the new variables

$$\begin{aligned} x(\tau) &= \exp\left[\mathcal{E}(\tau) - \mathcal{E}(\tau_0)\right], \\ y(\tau) &= \exp\left[\mathcal{N}(\tau) - \mathcal{N}(\tau_0)\right], \end{aligned} \tag{35}$$

with $x(\tau_0) = y(\tau_0) = 1$; and a_1 and a_2 are dimensionless constants determined by the initial conditions

$$\begin{aligned} a_1 &= eC\chi\left(\frac{n_{5,0}}{a}\right)^{1/3}\frac{B_0}{E_0}\tau_0, \\ a_2 &= \frac{e^2 C\chi E_0 B_0 \tau_0}{n_{5,0}}. \end{aligned} \tag{36}$$

Instead of solving Eqs. (23) and (27) or Eq. (31), now we only need to solve Eq. (27) with the initial condition $x(\tau_0) = y(\tau_0) = 1$. We see that both a_1 and a_2 are linearly proportional to the anomaly constant C, which is linearly proportional to the Planck constant. This means a_1 and a_2 are of quantum nature.

Now we try to solve Eq. (34) under some approximations. We can rewrite Eq. (34) in an integral form

$$\begin{aligned} x(\tau) &= e^{-\sigma(\tau-\tau_0)} - \frac{a_1}{\tau_0}e^{-\sigma\tau}\int_{\tau_0}^{\tau} d\tau' e^{\sigma\tau'}\left(\frac{\tau_0}{\tau'}\right)^{1/3} y^{1/3}(\tau'), \\ y(\tau) &= 1 + a_2\int_{\tau_0}^{\tau} d\tau'\frac{x(\tau')}{\tau'}. \end{aligned} \tag{37}$$

Since a_1 and a_2 terms are quantum corrections as a_1, $a_2 \propto \hbar$, we can deal with these terms as perturbations to the classical terms, so Eq. (34) or (37) can be solved order by order in powers of $\hbar$.

To the linear order in $\hbar$, we have the solutions for $x(\tau)$ and $y(\tau)$,

$$\begin{aligned} x(\tau) &= e^{-\sigma(\tau-\tau_0)} - \frac{a_1}{\tau_0^{2/3}}e^{-\sigma\tau}\left[\tau_0^{2/3}\mathrm{E}_{1/3}(-\sigma\tau_0) - \tau^{2/3}\mathrm{E}_{1/3}(-\sigma\tau)\right], \\ y(\tau) &= 1 + a_2\left[e^{\sigma\tau_0} - a_1\mathrm{E}_{1/3}(-\sigma\tau_0)\right]\left[\mathrm{E}_1(\sigma\tau_0) - \mathrm{E}_1(\sigma\tau)\right], \end{aligned}$$

where $\mathrm{E}_n(z) \equiv \int_1^\infty dt t^{-n}e^{-zt}$ is the generated exponential integral. Then we obtain the solutions for $E(\tau)$ and $n_5(\tau)$,

$$\begin{aligned} E(\tau) &= E_0\frac{\tau_0}{\tau}\left\{e^{-\sigma(\tau-\tau_0)} - \frac{a_1}{\tau_0^{2/3}}e^{-\sigma\tau}\left[\tau_0^{2/3}\mathrm{E}_{1/3}(-\sigma\tau_0)\right.\right. \\ &\quad \left.\left. - \tau^{2/3}\mathrm{E}_{1/3}(-\sigma\tau)\right]\right\}, \\ n_5(\tau) &= n_{5,0}\frac{\tau_0}{\tau}\left\{1 + a_2 e^{\sigma\tau_0}\left[\mathrm{E}_1(\sigma\tau_0) - \mathrm{E}_1(\sigma\tau)\right]\right\}. \end{aligned} \tag{38}$$

At early proper time, $\tau \to \tau_0$, we can expand $\mathrm{E}_n(\tau)$ near τ_0 and obtain

$$\begin{aligned} E(\tau) &\simeq E_0\frac{\tau_0}{\tau}\left[e^{-\sigma(\tau-\tau_0)} - \frac{a_1}{\tau_0}(\tau-\tau_0) + a_1\frac{1+3\tau_0\sigma}{6\tau_0^2}(\tau-\tau_0)^2\right], \\ n_5(\tau) &\simeq n_{5,0}\frac{\tau_0}{\tau}\left\{1 + a_2\frac{\tau-\tau_0}{\tau_0} - a_2\frac{1+\sigma\tau_0}{2\tau_0^2}(\tau-\tau_0)^2\right\}. \end{aligned} \tag{39}$$

Finally the energy density and the pressure can be solved by using the solutions for μ_5, E, B. From Eq. (25), we obtain the energy density

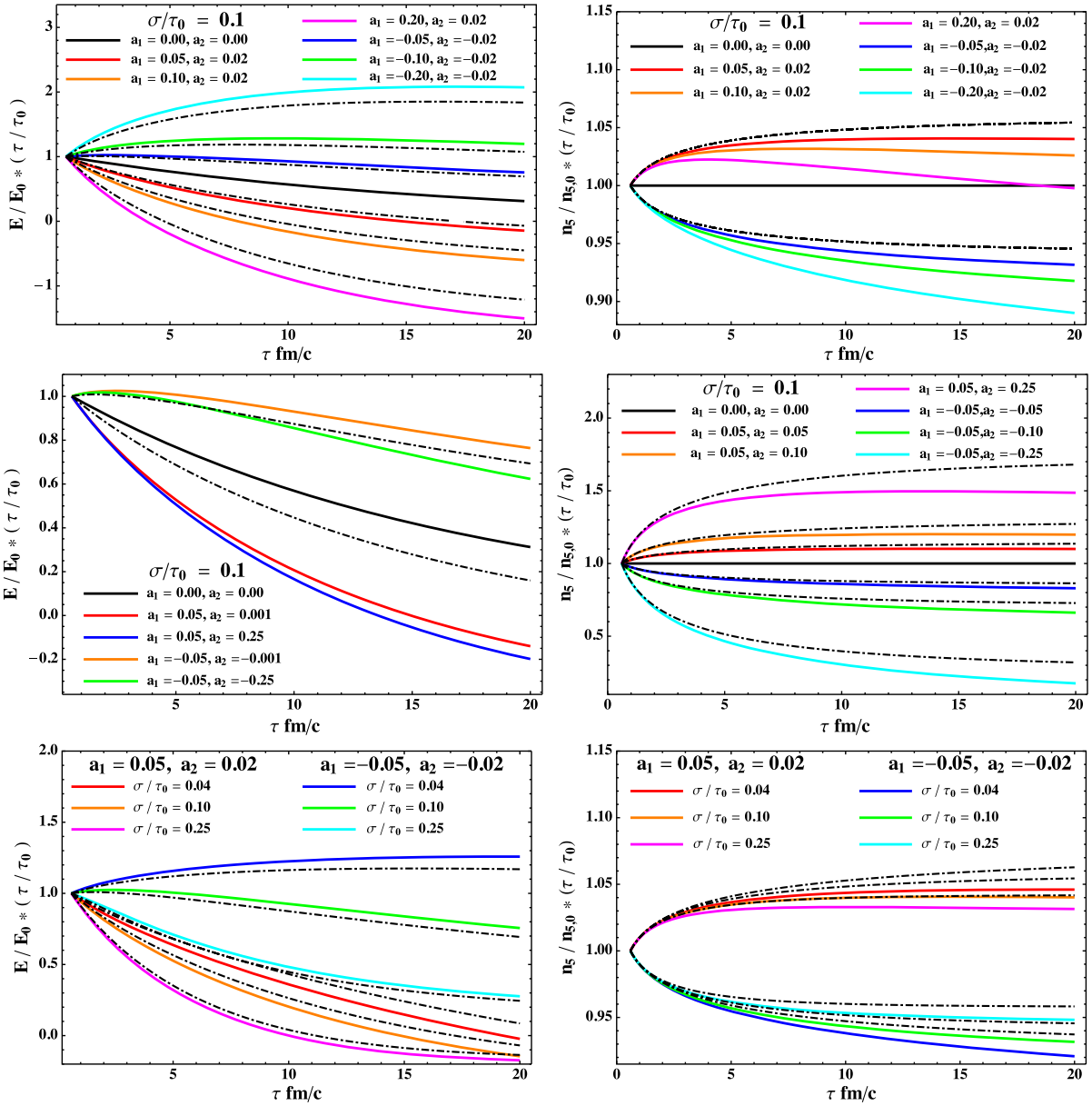

FIG. 1. The normalized electric field $E/E_0 \times (\tau/\tau_0)$ and chiral charge density $n_5/n_{5,0} \times (\tau/\tau_0)$ as functions of the proper time τ. We have chosen $\tau_0 = 0.6$ fm/c. The solid lines are obtained by solving Eq. (34) numerically and the dashed lines are from the approximate analytic solution (38). In the first row, we fix $\sigma/\tau_0 = 0.1$, $a_2 = \pm 0.2$ and change the values of a_1. In the second row, we fix $\sigma/\tau_0 = 0.1$, $a_1 = \pm 0.5$ and change the values of a_2. In the last row, we fix $(a_1, a_2) = \pm(0.05, 0.02)$ and change the values of σ/τ_0.

$$\varepsilon(\tau) = \varepsilon_0 \left(\frac{\tau_0}{\tau}\right)^{1+c_s^2} (1 + \Delta\varepsilon),$$
$$\Delta\varepsilon(\tau) = \frac{1}{\varepsilon_0} \int_{\tau_0}^{\tau} d\tau' \left(\frac{\tau'}{\tau_0}\right)^{1+c_s^2} [\sigma E^2(\tau') + \chi\xi(\tau') E(\tau') B(\tau')]. \tag{40}$$

We can also solve Eq. (34) numerically. We choose the initial proper time $\tau_0 = 0.6$ fm/c. The values of the electric conductivity vary in different situations. The lattice QCD calculations give $\sigma \sim 5.8T/T_c$ MeV [71–73], while in holographic QCD models it takes the value $\sigma \sim 20$–30 MeV for $T = 200$ MeV [21,23]. For σ in the weakly coupled QGP at finite temperature and chemical potential, see, e.g., Ref. [74]. In our numerical calculation, we choose $\sigma \sim 5$–30 MeV $\simeq 0.04 - 0.25\tau_0$.

In Fig. 1, we plot the normalized electric field $E/E_0 \times (\tau/\tau_0)$ and chiral charge density $n_5/n_{5,0} \times (\tau/\tau_0)$ as functions of the proper time τ. The solid lines are the numerical results from Eqs. (34), while the dashed lines are from the approximate analytic solution (38). Note that the approximate analytic solution for $E(\tau)$ is independent of a_2 and $n_5(\tau)$ independent of a_1 and σ. From these results, we see that the approximation works very well for small a_1 and a_2.

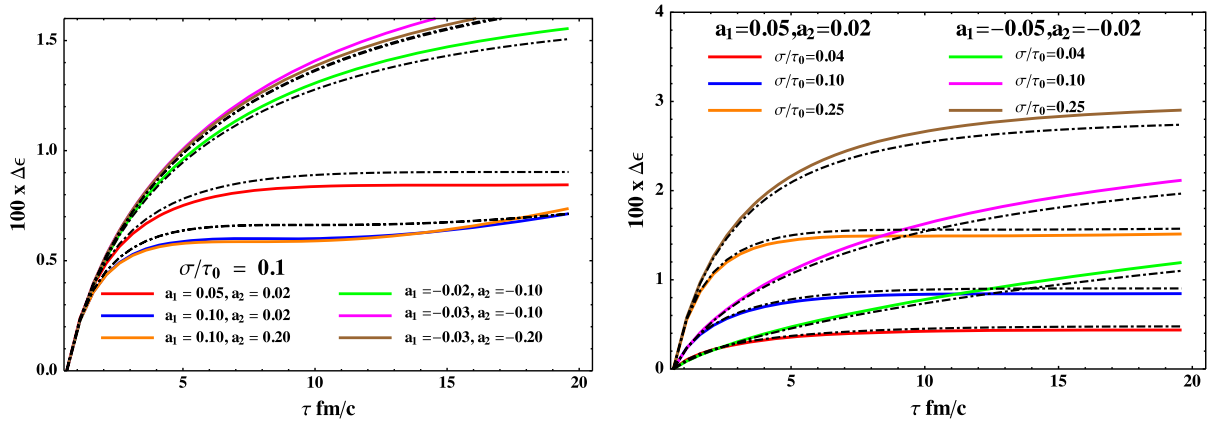

FIG. 2. The energy density correction $\Delta\varepsilon$ ($\times 100$) as functions of the proper time τ. The parameters are set to $\tau_0 = 0.6$ fm/c, $E_0^2/\epsilon_0 = 0.1$, $E_0 B_0/\epsilon_0 = 0.2$, $\mu_{5,0}/\tau_0 = 1$, and $c_s^2 = 1/3$. The solid lines are numerical solutions of Eq. (34) and the dashed lines are from the approximate analytic solution (38). In the left panel, we fix $\sigma/\tau_0 = 0.1$ and change the values of a_1 and a_2. In the right panel, we fix $(a_1, a_2) = \pm(0.05, 0.02)$ and change the values of σ/τ_0.

For positive a_1 and a_2, E decay faster as a_1 increases, while for negative a_1 and a_2, E decay slower as $|a_1|$ increases. For positive a_1 and a_2, n_5 decays slower as a_2 grows, while for negative a_1 and a_2, n_5 decays faster as $|a_2|$ grows. Such behaviors are obvious in the approximate analytic solution (38).

We observe that for large positive a_1 or large σ with positive a_1 and a_2, E/E_0 can be negative at late proper time. It means that the electric field flips its sign at the late time. From Eq. (38), one can see that a very large a_1 in the second term may dominate and make E/E_0 negative. Since a_1 is proportional to the initial chiral charge density, such a behavior may come from the competition between the anomalous conservation equation $\partial_\mu j_5^\mu = -CE \cdot B$ and Maxwell's equations.

One may expect that n_5 may have oscillation with time because it can be converted from the magnetic helicity and vice versa [61]. However, since the medium is expanding, the possible oscillation of n_5 is outperformed by its decay $n_5/n_{5,0} \sim \tau_0/\tau$.

In Fig. 2, we show the results of $\Delta\varepsilon$ in Eq. (40), which is amplified by a factor 100. The solid lines are numerical results from Eq. (34), while the dashed lines are given by the approximate analytic solution (38). Even with 100 times amplification of the difference, we see that the approximate analytic solution (38) still works well. For both positive and negative a_1 and a_2, $\Delta\varepsilon$ are positive because the first term dominates over the second one inside the square brackets in Eq. (40).

B. EoS (15)

For EoS (15), the equations for the energy density $\varepsilon(\tau)$, $E(\tau)$ and $n_5(\tau)$ are coupled together. We need to rewrite Eqs. (25), (23), and (27) as

$$\begin{aligned}
\frac{d}{d\tau}\varepsilon + (1+c_s^2)\varepsilon &= \varepsilon\frac{d}{d\tau}\mathcal{L}, \\
\frac{d}{d\tau}E + \frac{E}{\tau} &= E\frac{d}{d\tau}\mathcal{E}, \\
\frac{d}{d\tau}n_5 + \frac{n_5}{\tau} &= n_5\frac{d}{d\tau}\mathcal{N},
\end{aligned} \tag{41}$$

where

$$\begin{aligned}
\frac{d}{d\tau}\mathcal{L} &= \frac{1}{\varepsilon}\sigma E^2 + \frac{1}{\varepsilon}eC\chi\mu_5 EB, \\
\frac{d}{d\tau}\mathcal{E} &= -\sigma - eC\chi\mu_5\frac{B}{E}, \\
\frac{d}{d\tau}\mathcal{N} &= \frac{e^2 C\chi EB}{n_5}.
\end{aligned} \tag{42}$$

With the help of Eq. (29), the solutions are

$$\varepsilon(\tau) = \varepsilon_0\left(\frac{\tau_0}{\tau}\right)^{1+c_s^2}\exp\left[\mathcal{L}(\tau) - \mathcal{L}(\tau_0)\right], \tag{43}$$

and $n_5(\tau)$ and $E(\tau)$ are similar to Eq. (33).

From the EoS (15), one can express all thermodynamic quantities as functions of T and μ_5. Since the critical temperature $T_c \sim 200$ MeV is much larger than the chiral chemical potential in relativistic heavy ion collisions, i.e., $\mu_5 \ll T$, all terms proportional to μ_5 in the thermodynamic relations are negligible. As a consequence, we obtain

$$\varepsilon = \varepsilon_0\left(\frac{T}{T_0}\right)^{1+c_s^{-2}} + \mathcal{O}(\mu_5^2/T^2), \tag{44}$$

where $\varepsilon_0 = \varepsilon(\tau_0)$ and $T_0 = T(\tau_0)$. By introducing

$$x(\tau) = \exp[\mathcal{E}(\tau) - \mathcal{E}(\tau_0)],$$
$$y(\tau) = \exp[\mathcal{N}(\tau) - \mathcal{N}(\tau_0)],$$
$$z(\tau) = \exp[\mathcal{L}(\tau) - \mathcal{L}(\tau_0)], \tag{45}$$

Eq. (42) is reduced to

$$\frac{d}{d\tau}x = -\sigma x - \frac{a_1}{\tau_0}y(\tau)\left(\frac{\tau}{\tau_0}\right)^{-1+2c_s^2} z^{-2c_s^2/(1+c_s^2)},$$
$$\frac{d}{d\tau}y = a_2\frac{x(\tau)}{\tau},$$
$$\frac{d}{d\tau}z = \sigma\frac{E_0^2}{\varepsilon_0}\left(\frac{\tau_0}{\tau}\right)^{1-c_s^2}x^2(\tau) + \frac{a_3}{\tau_0}\left(\frac{\tau}{\tau_0}\right)^{-2+3c_s^2} \times x(\tau)y(\tau)z^{-2c_s^2/(1+c_s^2)}, \tag{46}$$

where $x(\tau_0) = y(\tau_0) = z(\tau_0) = 1$, and a_1, a_2 and a_3 are dimensionless constants determined by the initial conditions

$$a_1 = eC\chi\frac{B_0 n_{5,0}}{aT_0^2 E_0}\tau_0,$$
$$a_2 = \frac{e^2 C\chi E_0 B_0}{n_{5,0}}\tau_0,$$
$$a_3 = \frac{eC\chi}{a}\frac{n_{5,0}E_0 B_0}{\varepsilon_0 T_0^2}\tau_0. \tag{47}$$

These dimensionless constants are all linearly proportional to $\hbar$ through the anomaly constant C, which means they are of quantum nature. So we can deal with the terms proportional to a_1, a_2 and a_3 in Eq. (46) as perturbations to the classical terms, and Eq. (46) can be solved order by order in powers of $\hbar$.

To the linear order in $\hbar$, we have the solutions for $x(\tau)$, $y(\tau)$ and $z(\tau)$,

$$x(\tau) = e^{-\sigma(\tau-\tau_0)} - \frac{a_1}{\tau_0}e^{-\sigma\tau}\int_{\tau_0}^{\tau} d\tau' e^{\sigma\tau'}\left(\frac{\tau'}{\tau_0}\right)^{-1+2c_s^2}[z_0(\tau')]^{-2c_s^2/(1+c_s^2)},$$
$$y(\tau) = 1 + a_2 e^{\sigma\tau_0}[\mathrm{E}_1(\sigma\tau_0) - \mathrm{E}_1(\sigma\tau)],$$
$$z(\tau) = z_0(\tau) + \frac{a_3}{\tau_0}\int_{\tau_0}^{\tau} d\tau'\left(\frac{\tau'}{\tau_0}\right)^{-2+3c_s^2} e^{-\sigma(\tau'-\tau_0)}[z_0(\tau')]^{-2c_s^2/(1+c_s^2)}, \tag{48}$$

where

$$z_0(\tau) = 1 + \sigma\frac{E_0^2}{\varepsilon_0}e^{2\sigma\tau_0}\left[\tau_0\mathrm{E}_{1-c_s^2}(2\sigma\tau_0) - \tau\left(\frac{\tau}{\tau_0}\right)^{c_s^2-1}\mathrm{E}_{1-c_s^2}(2\sigma\tau')\right]. \tag{49}$$

We can further simplify the integration in $x(\tau)$ and $z(\tau)$. Since initial energy density ε_0 is much larger than the initial energy of the EM fields $\varepsilon_0 \gg B_0^2$, E_0^2, E_0B_0 (see, e.g., Ref. [34] for the values of B_0^2/ε_0 in the event-by-event simulation of relativistic heavy ion collisions), we can further simplify the integration in $x(\tau)$ and $z(\tau)$ in the linear order in E_0^2/ε_0 as

$$x(\tau) = e^{-\sigma(\tau-\tau_0)} - \frac{a_1}{\tau_0}e^{-\sigma\tau}\left[\tau_0\mathrm{E}_{1-2c_s^2}(-\sigma\tau_0) - \tau\left(\frac{\tau}{\tau_0}\right)^{-1+2c_s^2}\mathrm{E}_{1-2c_s^2}(-\sigma\tau)\right] + \mathcal{O}(a_i^2, a_i E_0^2/\varepsilon_0),$$
$$z(\tau) = 1 + \sigma\frac{E_0^2}{\varepsilon_0}e^{2\sigma\tau_0}\left[\tau_0\mathrm{E}_{1-c_s^2}(2\sigma\tau_0) - \tau\left(\frac{\tau}{\tau_0}\right)^{c_s^2-1}\mathrm{E}_{1-c_s^2}(2\sigma\tau)\right] + \frac{a_3}{\tau_0}e^{\sigma\tau_0}\left[\tau_0\mathrm{E}_{2-3c_s^2}(\sigma\tau_0) - \tau\left(\frac{\tau_0}{\tau}\right)^{2-3c_s^2}\mathrm{E}_{2-3c_s^2}(\sigma\tau)\right] + \mathcal{O}(a_i^2, a_i E_0^2/\varepsilon_0). \tag{50}$$

Then we obtain the solutions for $E(\tau)$, $n_5(\tau)$ and $\varepsilon(\tau)$ in the linear order in $\hbar$ and E_0^2/ε_0,

$$E(\tau) = E_0\left(\frac{\tau_0}{\tau}\right)\left\{e^{-\sigma(\tau-\tau_0)} - a_1 e^{-\sigma\tau}\left[\mathrm{E}_{1-2c_s^2}(-\sigma\tau_0) - \left(\frac{\tau}{\tau_0}\right)^{2c_s^2}\mathrm{E}_{1-2c_s^2}(-\sigma\tau)\right]\right\},$$
$$n_5(\tau) = n_{5,0}\left(\frac{\tau_0}{\tau}\right)\{1 + a_2 e^{\sigma\tau_0}[\mathrm{E}_1(\sigma\tau_0) - \mathrm{E}_1(\sigma\tau)]\},$$
$$\varepsilon(\tau) = \epsilon_0\left(\frac{\tau_0}{\tau}\right)^{1+c_s^2}\left\{1 + \sigma\frac{E_0^2}{\varepsilon_0}e^{2\sigma\tau_0}\left[\tau_0\mathrm{E}_{1-c_s^2}(2\sigma\tau_0) - \tau\left(\frac{\tau}{\tau_0}\right)^{c_s^2-1}\mathrm{E}_{1-c_s^2}(2\sigma\tau')\right] + \frac{a_3}{\tau_0}e^{\sigma\tau_0}\left[\tau_0\mathrm{E}_{2-3c_s^2}(\sigma\tau_0) - \tau\left(\frac{\tau_0}{\tau}\right)^{2-3c_s^2}\mathrm{E}_{2-3c_s^2}(\sigma\tau)\right]\right\}. \tag{51}$$

In the leading order, we see $E(\tau) \sim \frac{\tau_0}{\tau} x(\tau) \sim \frac{1}{\tau} e^{-\sigma\tau}$, i.e., the electric field decays in the conducting medium [69]. In the leading order, $y(\tau) \sim 1$ means $n_5 \sim \frac{\tau_0}{\tau}$. We also see that when $c_s^2 = 1/3$, the analytic solutions of $E(\tau)$ and $n_5(\tau)$ have the same form as in Eq. (38) in the previous subsection.

In Figs. 3–5, we plot the normalized $E/E_0 \times (\tau/\tau_0)$, $n_5/n_{5,0} \times (\tau/\tau_0)$ and $\varepsilon/\varepsilon_0 \times (\tau/\tau_0)^{1+c_s^2}$ as functions of the proper time τ. We choose the $\tau_0 = 0.6$ fm/c, the speed of sound $c_s^2 = 1/3$ and $E_0^2/\varepsilon_0 = 0.1$. The solid lines in those figures are the numerical results from Eqs. (46), while the dashed lines are from approximate analytic solutions (51). We see that the approximation works very well for small a_i.

In Fig. 3, we find E/E_0 is almost independent of a_2 and a_3, as expected in Eq. (51). The E/E_0 decays rapidly as a_1 or σ grows. Similar to the cases in Sec. IV A, E/E_0 can be negative at the late proper time. Such a behavior may come from the competition between the anomalous conservation equation $\partial_\mu j_5^\mu = -CE \cdot B$ and Maxwell's equations.

In Fig. 4, the numerical results show that n_5 is almost independent of a_1 and a_3 in small a_i cases as expected in Eq. (51). The n_5 decays slowly as a_2 increases and the decay behavior of n_5 is also not sensitive to variation of σ.

In Fig. 5, we find that the time evolution of $\varepsilon(\tau)$ seems to be insensitive to a_1 and a_2. Because $E_0^2/\varepsilon_0 \ll 1$, the contribution from the second term in Eq. (51) which is proportional to $\sigma E_0^2/\varepsilon_0$ is negligible. Interestingly, the energy density decays slower as a_3 grows. As shown in Fig. 5, for a large value of a_3, e.g., $a_3 = 3.0$, the energy density even increases at early time. That is because the fluid gains the energy from the EM fields; i.e., the a_3 term in Eq. (51) dominates. Similar behavior is also found in the ideal MHD with a background magnetic field [54,55].

We make some remarks here. From analytic solutions (38) and (51), we conclude that the CME and chiral anomaly as quantum corrections play a role to the time evolution of the electric field $E(\tau)$, the chiral charge density $n_5(\tau)$ and the energy density $\varepsilon(\tau)$. With an initial magnetic field parallel to the electric field (with $\chi = 1$) and all a_i ($i = 1, 2, 3$) being positive, $E(\tau)/n_5(\tau)$ decay faster/slower than the cases without CME. If the initial magnetic field is antiparallel to the electric field (with $\chi = -1$) and all a_i are negative, $E(\tau)/n_5(\tau)$ decay slower/faster than the cases without CME. This behavior is consistent with the anomalous conservation equation $\partial_\mu j_5^\mu = -CE^\mu B_\mu = C\chi E(\tau)B(\tau)$ combined with Maxwell's

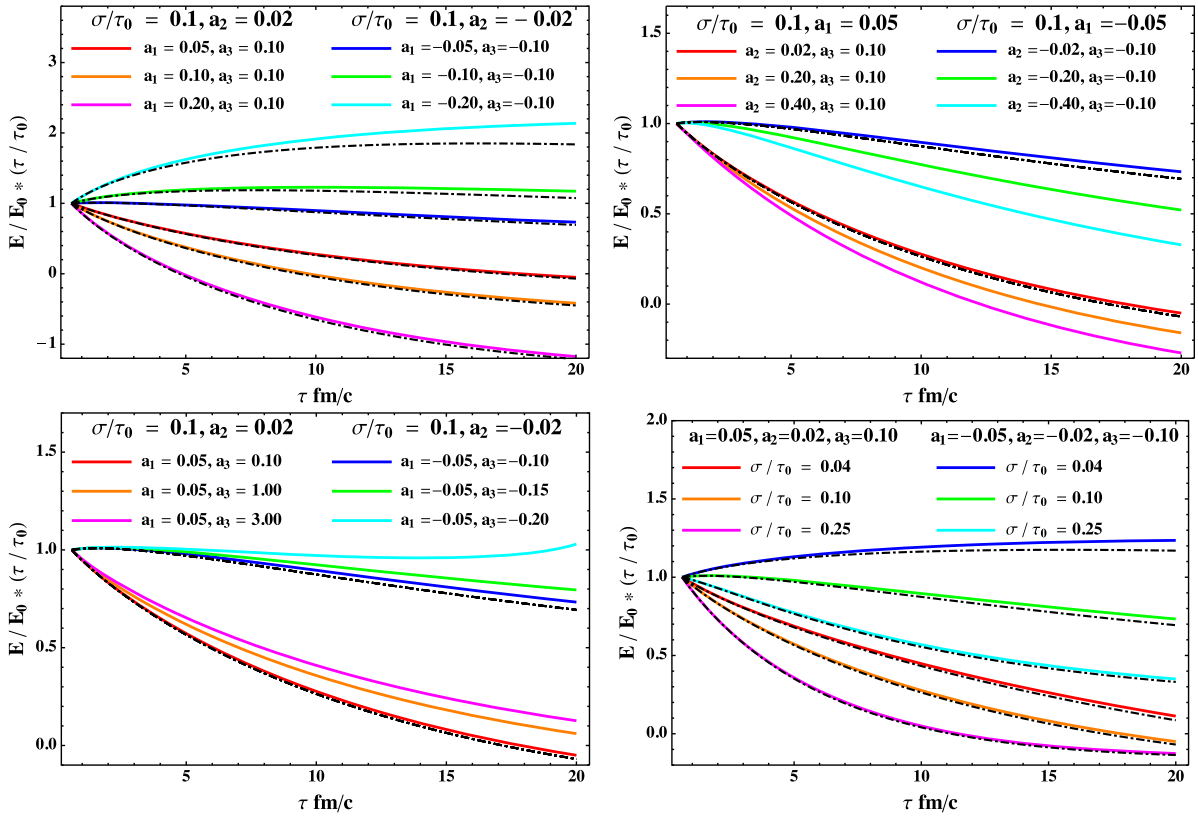

FIG. 3. The normalized electric field $E/E_0 \times (\tau/\tau_0)$ as functions of the proper time τ. We have chosen $\tau_0 = 0.6$ fm/c, $c_s^2 = 1/3$ and $E_0^2/\varepsilon_0 = 0.1$. The solid lines are obtained by solving Eq. (46) numerically and the dashed lines are from the approximate analytic solution (51). In the first row, we fix $\sigma/\tau_0 = 0.1$, $a_2 = \pm 0.2$, $a_3 = \pm 0.10$ and change the values of a_1. In the second row, we fix $\sigma/\tau_0 = 0.1$, $a_1 = \pm 0.5$ and change the values of a_2. In the last row, we fix $(a_1, a_2) = \pm(0.05, 0.02)$ and change the values of σ/τ_0.

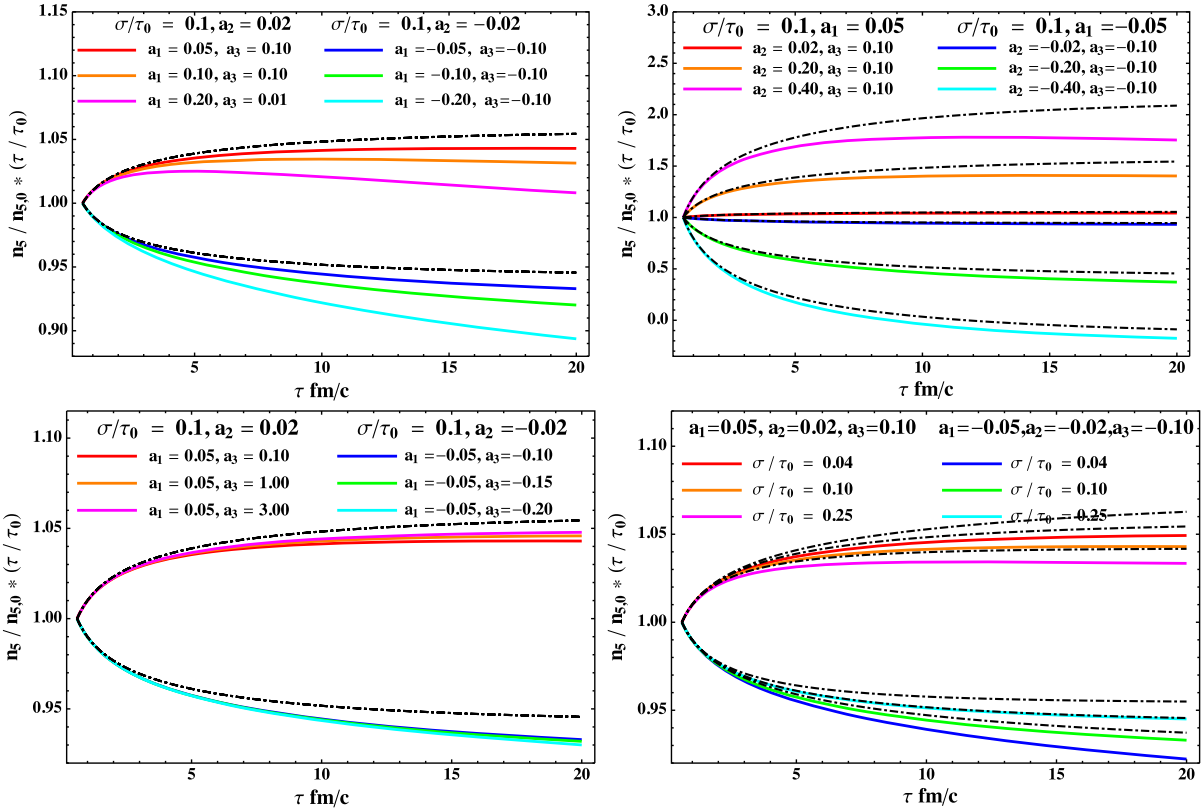

FIG. 4. The normalized chiral charge density $n_5/n_{5,0} \times (\tau/\tau_0)$ as functions of the proper time τ. We have chosen $\tau_0 = 0.6$ fm/c, $c_s^2 = 1/3$ and $E_0^2/\varepsilon_0 = 0.1$. The solid lines are obtained by solving Eq. (46) numerically and the dashed lines are from the approximate analytic solution (51). In the first row, we fix $\sigma/\tau_0 = 0.1$, $a_2 = \pm 0.2$, $a_3 = \pm 0.10$ and change the values of a_1. In the second row, we fix $\sigma/\tau_0 = 0.1$, $a_1 = \pm 0.5$ and change the values of a_2.

equations. For example, if $\chi = +1$, we have $\partial_\tau(n_5\tau) = C\tau\chi E(\tau)B(\tau) > 0$, implying that $n_5(\tau)$ decays slower than the case $C = 0$. From Eq. (23), we have $\partial_\tau[E\tau\exp(\sigma\tau)] = -\tau\chi\xi B(\tau) < 0$; i.e., $E(\tau)$ decays faster than the case $C = 0$. Such a behavior is due to the chiral charge density being converted from the magnetic helicity. For $\chi = -1$, the magnetic helicity is converted from the chiral charge density so the behavior is opposite. The numerical results in Figs. 1–5 are consistent with the above observation.

So far, we have only discussed the time evolution of EM fields and thermodynamic quantities in the presence of CME and chiral anomaly. From our results, it is hard to see how these effects will affect the final states in the relativistic heavy ion collisions since the modifications from these quantum effects are not significant. It implies that the contributions from these quantum effects to the quantities in the experiments, which have already been fitted well from the ordinary hydrodynamic simulations, such as elliptic flow v_2, might be negligible. However, on the other hand, these quantum effects might contribute to the quantities related to CME or charge separation, e.g., asymmetric azimuthal charged particle correlations [36,37]. Confirming that requires the systematic numerical studies with the suitable initial conditions and EoS. For the discussion related to the heavy ion experiments, we refer to two studies in Refs. [75,76], of which the magnetic fields are considered as background fields.

C. Discussions

In Secs. IV A and IV B, we have obtained the approximate analytic solutions in two types of EoS. From Eq. (30), the proper time behavior of the magnetic field seems to be the same as the case without CME and finite conductivity, i.e., in an ideal MHD [54–56]. It seems to be counterintuitive and inconsistent with Maxwell's equations. Our explanation is as follows. The E^μ and B^μ defined in the four vector form of EM fields in Eq. (5) are the fields in the comoving frame of the fluid. The $B(\tau)$ in Eq. (30) is the length of the magnetic field three vector $\mathbf{B}$. The corrections from CME and finite conductivity to EM field can be shown after we transfer EM fields from co-moving frame to the laboratory frame.

From Eq. (4), we observe that the EM field strength tensor $F^{\mu\nu}$ as well as the energy-momentum tensor $T^{\mu\nu}$ and fluid velocity u^μ is measured in the laboratory frame. According to the standard definitions of EM fields through the field strength tensor $F^{\mu\nu}$, i.e.,

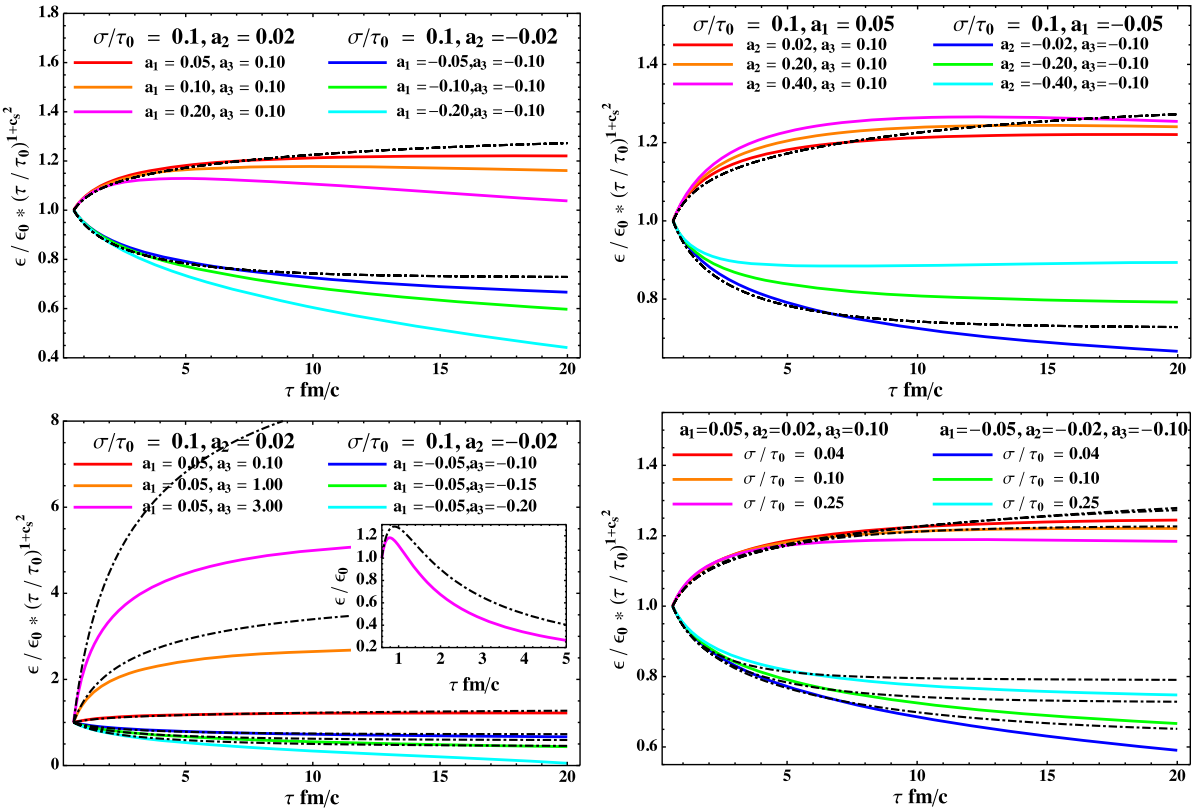

FIG. 5. The normalized energy density $\varepsilon/\varepsilon_0 \times (\tau/\tau_0)^{1+c_s^2}$ as functions of the proper time τ. We have chosen $\tau_0 = 0.6$ fm/c, $c_s^2 = 1/3$ and $E_0^2/\varepsilon_0 = 0.1$. The solid lines are obtained by solving Eq. (46) numerically and the dashed lines are from the approximate analytic solution (51). In the first row, we fix $\sigma/\tau_0 = 0.1$, $a_2 = \pm 0.2$, $a_3 = \pm 0.10$ and change the values of a_1. In the second row, we fix $\sigma/\tau_0 = 0.1$, $a_1 = \pm 0.5$ and change the values of a_2.

$$\mathbf{E}_L^i = F^{i0}, \qquad \mathbf{B}_L^i = -\frac{1}{2}\epsilon^{ijk}F^{jk},$$

we can get the EM fields in the lab frame

$$\mathbf{E}_L = (\gamma v^z B(\tau), \chi\gamma E(\tau), 0),$$
$$\mathbf{B}_L = (-\gamma v^z \chi E(\tau), \gamma B(\tau), 0), \tag{52}$$

where in this subsection, we use the lower index L for the EM fields in the laboratory frame and $E(\tau)$ and $B(\tau)$ are the functions solved in previous Sec. IV. We find that in the lab frame $\mathbf{B}_L^x$ and $\mathbf{E}_L^y$ depend on the finite conductivity σ and CME coefficient ξ through $E(\tau)$.

Next, we check the self-consistence of Maxwell's equations. We prove that the CME and finite conducting current do not generate the EM fields in the z direction, i.e., $\mathbf{E}_L^z$ and $\mathbf{B}_L^z$ are always vanishing. From

$$\nabla \times \mathbf{E}_L = -\partial_t \mathbf{B}_L, \tag{53}$$

we observe that with Eq. (52) the $\partial_t \mathbf{B}_L^z = 0$ and $\partial_y \mathbf{E}_L^z = -\partial_t \mathbf{B}_L^x + \partial_z \mathbf{E}_L^y = 0$ are automatically satisfied. With the solution (30), we can also obtain that $\partial_x \mathbf{E}_L^z = \partial_t \mathbf{B}_L^y + \partial_z \mathbf{E}_L^x = 0$.

Similarly from

$$\nabla \cdot \mathbf{E}_L = n_e, \qquad \nabla \cdot \mathbf{B}_L = 0, \tag{54}$$

and Eq. (52), we can also obtain that $\partial_z \mathbf{E}_L^z = -\partial_x \mathbf{E}_L^x - \partial_y \mathbf{E}_L^y = 0$ with $n_e = 0$, and $\partial_z \mathbf{B}_L^z = -\partial_x \mathbf{B}_L^x - \partial_y \mathbf{B}_L^y = 0$.

We focus on the last equation,

$$\nabla \times \mathbf{B}_L = \mathbf{j}_e + \partial_t \mathbf{E}_L. \tag{55}$$

Different from the charge current in a static conductor, the charge current $\mathbf{j}_e$ of a relativistic fluid includes two parts. The part parallel to the fluid velocity u^μ reads

$$\mathbf{j}_{e,\parallel} = \sigma \mathbf{E}_{L,\parallel} + \xi \mathbf{B}_{L,\parallel}, \tag{56}$$

and the other part perpendicular to the fluid velocity is given by

$$\mathbf{j}_{e,\perp} = \sigma\gamma(\mathbf{E}_L + \mathbf{v} \times \mathbf{B}_L)_\perp + \xi\gamma(\mathbf{B}_L - \mathbf{v} \times \mathbf{E}_L)_\perp, \tag{57}$$

with $\mathbf{v}$ being the three vector of fluid velocity, i.e., $u^\mu = \gamma(1, \mathbf{v})$. In our case, since the fluid moves along the z direction, the charge current is given by

$$\mathbf{j}_e = [\gamma(\mathbf{E}_L^y + v^z \mathbf{B}_L^x) + \xi\gamma(\mathbf{B}_L^y - v^z \mathbf{E}_L^x)]\mathbf{e}_y. \tag{58}$$

With Eq. (52), we find that $\partial_y \mathbf{B}_L^z = \partial_t \mathbf{E}_L^x + \partial_z \mathbf{B}_L^y = 0$ and $\partial_t \mathbf{E}_L^z = 0$. The space derivative of magnetic field in the z direction is

$$\partial_x \mathbf{B}_L^z = \partial_z \mathbf{B}_L^x - \sigma\gamma(\mathbf{E}_L^y + v^z \mathbf{B}_L^x) - \xi\gamma(\mathbf{B}_L^y - v^z \mathbf{E}_L^x) - \partial_t \mathbf{E}_L^y, \tag{59}$$

where the left-handed side of the above equation is equal to the right-handed side of Eq. (23). Thus, inserting our solutions in Eqs. (38) and (51) yields $\partial_x \mathbf{B}_L^z = 0$.

Since both time and space derivatives of $\mathbf{E}_L^z$ and $\mathbf{B}_L^z$ vanish and initial $\mathbf{E}_L^z$ or $\mathbf{B}_L^z$ are chosen to be vanishing, we can conclude that in our setup the CME and conducting current will not generate EM fields in the z direction in the lab frame. Whereas only the space-time derivatives of EM fields in the transverse direction, e.g., $\mathbf{B}_L^x$ and $\mathbf{E}_L^y$, are nonvanishing. This is quite different from the case of static media, in which the CME current can induce a circular magnetic field [61].

Thirdly, we discuss the Bjorken fluid velocity. Usually, we can consider the right-handed side of Eq. (26) as the covariant form of Lorentz force acting on the fluid. In the lab frame, we can rewrite it as

$$F^{\nu\lambda} j_{e\lambda} = (j_{e,0}\mathbf{E}_L, \mathbf{j}_e \times \mathbf{B}_L). \tag{60}$$

Since we have chosen the $\mu_e = 0$, the electric field will not accelerate the fluid, i.e., the zeroth component $j_{e,0}\mathbf{E}_L = 0$. The other component $\mathbf{j}_e \times \mathbf{B}_L$ is the Lorentz force driving by the magnetic field, where $\mathbf{j}_e$ is given by Eqs. (56) and (57). In our case, the EM fields with Lorentz force $\mathbf{j}_e \times \mathbf{B}_L$ are analogous to the so-called force-free fields (e.g., also see the discussion in the classical electrodynamics [62,63] and recent studies in Refs. [77,78]). Through Eqs. (19) and (25), we have already shown that the EM fields in our setup will not modify the fluid velocity.

At last, we check the consistence of (anomalous) current conservation equations. Since Eqs. (38) and (51) are the solutions of anomalous current equation $\partial_\mu j_5^\mu = -CE \cdot B$, the anomalous current equation should be satisfied. Because EM fields are independent of x, y, the charge current conservation equation reduces to $\partial_\mu j_e^\mu = \partial_t j_{e,0} + \nabla \cdot \mathbf{j}_e = \partial_z \mathbf{j}_{e,z}$, with $\mathbf{j}_{e,z} = \mathbf{j}_{e,\parallel} = \sigma \mathbf{E}_{L,z} + \xi \mathbf{B}_{L,z} = 0$. We can conclude that the (anomalous) current conservation equations are satisfied.

Before we end this section, we make some remarks here. We have computed the EM fields in the lab frame and found that our solutions satisfy Maxwell's equations. In our setup, the CME and electric conducting current do not generate the EM fileds in the z direction in lab frame. It is quite different from the case in static media. We have also shown that the Lorentz force does not accelerate the fluid. At last, we have checked the self-consistence of (anomalous) current conservation equations.

V. SUMMARY AND CONCLUSIONS

We have solved MHD equations with longitudinal boost invariance and transverse EM fields in the presence of the CME and finite electric conductivity. The MHD equations involve the energy momentum, the electric charge and chiral charge (anomalous) conservation equations coupled with Maxwell's equations. We consider two types of EoS corresponding to the large chiral chemical potential and the high temperature cases, respectively. For further simplification, we assume that the fluid is electric charge neutral, i.e., we set the electric charge density n_e and electric charge chemical potential μ_e vanish.

We assume the Bjorken form of the fluid velocity in the longitudinal direction. To keep the fluid velocity unchanged, we obtain the four-vector form of the electric and magnetic field, which are orthogonal to the fluid velocity. To solve the MHD equations, we treat the terms with the anomaly constant which is proportional to the Planck constant $\hbar$ as perturbations. This is equivalent to an expansion in $\hbar$. Then we apply the nonconserved charge method to obtain the approximate analytic solutions. The comparison of the analytic solutions with the exact numerical results shows good agreement.

Finally we compute the EM field in three-vector form in the lab frame and show the contributions from the electric conductivity and the CME. According to Maxwell's equations, in our setup, the CME and electrically conducting current only modify the EM fields in the transverse direction in the lab frame. The electric and magnetic field in the z direction does not grow with time and space. The Lorentz force only changes the time evolution of thermodynamic quantities and does not accelerate the fluid.

Our results can provide a future test of complete numerical simulations of the MHD with the CME. Since the polarization of chiral fermions in the strong magnetic field is different from the ordinary magnetization which is called the chiral Barnett effect [79], the current method can be applied to study the magnetization effect in the future.

ACKNOWLEDGMENTS

S. P. thanks Masoud Shokri and Duan Yu for helpful discussions. Q. W. is supported in part by the National Natural Science Foundation of China (NSFC) under Grants No. 11535012 and No. 11890713, the 973 program under Grant No. 2015CB856902, and the Key Research Program of the Chinese Academy of Sciences under Grant No. XDPB09. S. P. is supported by One Thousand Talent Program for Young Scholars. I. S. is supported by the Chinese Academy of Sciences and The World Academy of Sciences (CAS-TWAS) scholarship.

[1] A. Vilenkin, Phys. Rev. D **22**, 3080 (1980).
[2] D. E. Kharzeev, L. D. McLerran, and H. J. Warringa, Nucl. Phys. **A803**, 227 (2008).
[3] K. Fukushima, D. E. Kharzeev, and H. J. Warringa, Phys. Rev. D **78**, 074033 (2008).
[4] M. Stephanov and Y. Yin, Phys. Rev. Lett. **109**, 162001 (2012).
[5] J.-W. Chen, J.-y. Pang, S. Pu, and Q. Wang, Phys. Rev. D **89**, 094003 (2014).
[6] J.-Y. Chen, D. T. Son, M. A. Stephanov, H.-U. Yee, and Y. Yin, Phys. Rev. Lett. **113**, 182302 (2014).
[7] D. T. Son and N. Yamamoto, Phys. Rev. Lett. **109**, 181602 (2012).
[8] D. T. Son and N. Yamamoto, Phys. Rev. D **87**, 085016 (2013).
[9] J.-H. Gao, Z.-T. Liang, S. Pu, Q. Wang, and X.-N. Wang, Phys. Rev. Lett. **109**, 232301 (2012).
[10] J.-W. Chen, S. Pu, Q. Wang, and X.-N. Wang, Phys. Rev. Lett. **110**, 262301 (2013).
[11] J.-h. Gao and Q. Wang, Phys. Lett. B **749**, 542 (2015).
[12] Y. Hidaka, S. Pu, and D.-L. Yang, Phys. Rev. D **95**, 091901 (2017).
[13] Y. Hidaka, S. Pu, and D.-L. Yang, Phys. Rev. D **97**, 016004 (2018).
[14] J.-h. Gao, S. Pu, and Q. Wang, Phys. Rev. D **96**, 016002 (2017).
[15] Y. Hidaka, S. Pu, and D.-L. Yang, Nucl. Phys. **A982**, 547 (2019).
[16] J.-H. Gao, Z.-T. Liang, Q. Wang, and X.-N. Wang, Phys. Rev. D **98**, 036019 (2018).
[17] A. Huang, S. Shi, Y. Jiang, J. Liao, and P. Zhuang, Phys. Rev. D **98**, 036010 (2018).
[18] N. Mueller and R. Venugopalan, Phys. Rev. D **96**, 016023 (2017).
[19] N. Mueller and R. Venugopalan, Phys. Rev. D **97**, 051901 (2018).
[20] X.-G. Huang and J. Liao, Phys. Rev. Lett. **110**, 232302 (2013).
[21] S. Pu, S.-Y. Wu, and D.-L. Yang, Phys. Rev. D **89**, 085024 (2014).
[22] Y. Jiang, X.-G. Huang, and J. Liao, Phys. Rev. D **91**, 045001 (2015).
[23] S. Pu, S.-Y. Wu, and D.-L. Yang, Phys. Rev. D **91**, 025011 (2015).
[24] K. Fukushima, D. E. Kharzeev, and H. J. Warringa, Phys. Rev. Lett. **104**, 212001 (2010).
[25] H. J. Warringa, Phys. Rev. D **86**, 085029 (2012).
[26] P. Copinger, K. Fukushima, and S. Pu, Phys. Rev. Lett. **121**, 261602 (2018).
[27] X.-L. Sheng, R.-H. Fang, Q. Wang, and D. H. Rischke, Phys. Rev. D **99**, 056004 (2019).
[28] A. Bzdak, V. Koch, and J. Liao, Lect. Notes Phys. **871**, 503 (2013).
[29] K. Fukushima, Lect. Notes Phys. **871**, 241 (2013).
[30] D. E. Kharzeev, Prog. Part. Nucl. Phys. **75**, 133 (2014).
[31] D. E. Kharzeev, Annu. Rev. Nucl. Part. Sci. **65**, 193 (2015).
[32] A. Bzdak and V. Skokov, Phys. Lett. B **710**, 171 (2012).
[33] W.-T. Deng and X.-G. Huang, Phys. Rev. C **85**, 044907 (2012).
[34] V. Roy and S. Pu, Phys. Rev. C **92**, 064902 (2015).
[35] H. Li, X.-l. Sheng, and Q. Wang, Phys. Rev. C **94**, 044903 (2016).
[36] B. Abelev *et al.* (STAR Collaboration), Phys. Rev. Lett. **103**, 251601 (2009).
[37] B. Abelev *et al.* (STAR Collaboration), Phys. Rev. C **81**, 054908 (2010).
[38] V. Khachatryan *et al.* (CMS Collaboration), Phys. Rev. Lett. **118**, 122301 (2017).
[39] A. M. Sirunyan *et al.* (CMS Collaboration), Phys. Rev. C **97**, 044912 (2018).
[40] V. Koch, S. Schlichting, V. Skokov, P. Sorensen, J. Thomas, S. Voloshin, G. Wang, and H.-U. Yee, Chin. Phys. C **41**, 072001 (2017).
[41] S. Ebihara, K. Fukushima, and S. Pu, Phys. Rev. D **96**, 016016 (2017).
[42] Y. Sun, C. M. Ko, and F. Li, Phys. Rev. C **94**, 045204 (2016).
[43] A. Huang, Y. Jiang, S. Shi, J. Liao, and P. Zhuang, Phys. Lett. B **777**, 177 (2018).
[44] M. Mace, S. Schlichting, and R. Venugopalan, Phys. Rev. D **93**, 074036 (2016).
[45] M. Mace, N. Mueller, S. Schlichting, and S. Sharma, Phys. Rev. D **95**, 036023 (2017).
[46] J. Berges, M. Mace, and S. Schlichting, Phys. Rev. Lett. **118**, 192005 (2017).
[47] P. Romatschke and U. Romatschke, Phys. Rev. Lett. **99**, 172301 (2007).
[48] M. Luzum and P. Romatschke, Phys. Rev. C **78**, 034915 (2008).
[49] H. Song and U. W. Heinz, Phys. Lett. B **658**, 279 (2008).
[50] H. Song and U. W. Heinz, Phys. Rev. C **78**, 024902 (2008).
[51] B. Schenke, S. Jeon, and C. Gale, Phys. Rev. C **85**, 024901 (2012).
[52] V. Roy, A. K. Chaudhuri, and B. Mohanty, Phys. Rev. C **86**, 014902 (2012).
[53] H. Niemi, G. S. Denicol, P. Huovinen, E. Molnar, and D. H. Rischke, Phys. Rev. C **86**, 014909 (2012).
[54] S. Pu, V. Roy, L. Rezzolla, and D. H. Rischke, Phys. Rev. D **93**, 074022 (2016).
[55] V. Roy, S. Pu, L. Rezzolla, and D. Rischke, Phys. Lett. B **750**, 45 (2015).
[56] S. Pu and D.-L. Yang, Phys. Rev. D **93**, 054042 (2016).
[57] S. Pu and D.-L. Yang, EPJ Web Conf. **137**, 13021 (2017).
[58] V. Roy, S. Pu, L. Rezzolla, and D. H. Rischke, Phys. Rev. C **96**, 054909 (2017).
[59] M. Shokri and N. Sadooghi, J. High Energy Phys. 11 (2018) 181.
[60] G. Inghirami, L. Del Zanna, A. Beraudo, M. H. Moghaddam, F. Becattini, and M. Bleicher, Eur. Phys. J. C **76**, 659 (2016).
[61] Y. Akamatsu and N. Yamamoto, Phys. Rev. Lett. **111**, 052002 (2013).
[62] S. Chandrasekhar and L. Woltjer, Proc. Natl. Acad. Sci. U.S.A. **44**, 285 (1958).
[63] L. Woltjer, Proc. Natl. Acad. Sci. U.S.A. **44**, 489 (1958).
[64] M. M. Caldarelli, O. J. C. Dias, and D. Klemm, J. High Energy Phys. 03 (2009) 025.
[65] M. Gedalin and I. Oiberman, Phys. Rev. E **51**, 4901 (1995).
[66] X.-G. Huang, M. Huang, D. H. Rischke, and A. Sedrakian, Phys. Rev. D **81**, 045015 (2010).
[67] S. Pu, arXiv:1108.5828.

[68] J. D. Bjorken, Phys. Rev. D **27**, 140 (1983).
[69] M. Shokri and N. Sadooghi, Phys. Rev. D **96**, 116008 (2017).
[70] T. Csorgo, F. Grassi, Y. Hama, and T. Kodama, Phys. Lett. B **565**, 107 (2003).
[71] G. Aarts, C. Allton, J. Foley, S. Hands, and S. Kim, Phys. Rev. Lett. **99**, 022002 (2007).
[72] H. T. Ding, A. Francis, O. Kaczmarek, F. Karsch, E. Laermann, and W. Soeldner, Phys. Rev. D **83**, 034504 (2011).
[73] K. Tuchin, Adv. High Energy Phys. **2013**, 490495 (2013).
[74] J.-W. Chen, Y.-F. Liu, S. Pu, Y.-K. Song, and Q. Wang, Phys. Rev. D **88**, 085039 (2013).
[75] Y. Jiang, S. Shi, Y. Yin, and J. Liao, Chin. Phys. C **42**, 011001 (2018).
[76] S. Shi, Y. Jiang, E. Lilleskov, and J. Liao, Ann. Phys. (Amsterdam) **394**, 50 (2018).
[77] H. Qin, W. Liu, H. Li, and J. Squire, Phys. Rev. Lett. **109**, 235001 (2012).
[78] X.-l. Xia, H. Qin, and Q. Wang, Phys. Rev. D **94**, 054042 (2016).
[79] K. Fukushima, S. Pu, and Z. Qiu, Phys. Rev. A **99**, 032105 (2019).